Generic Relevance of Counter Charges for Cation-Based Nanoscale Resistive Switching Memories

Stefan Tappertzhofen,[†,‡] Ilia Valov,[†,‡,§,*] Tohru Tsuruoka,[⊥] Tsuyoshi Hasegawa,[⊥] Rainer Waser,[†,‡,§] and Masakazu Aono[⊥]

[†]Institut für Werkstoffe der Elektrotechnik 2, RWTH Aachen University, 52074 Aachen, Germany, [‡]JARA-FIT, Fundamentals of Future Information Technology, 52425 Jülich, Germany, [§]Peter Grünberg Institut 7, Forschungszentrum Jülich GmbH, 52425 Jülich, Germany, and [⊥]International Center for Materials Nanoarchitectonics (MANA), National Institute for Materials Science (NIMS), 1-1 Namiki, 305-0044 Tsukuba, Japan

ABSTRACT Resistive switching memories (ReRAMs) are the major candidates for replacing the state-of-the-art memory technology in future nanoelectronics. These nonvolatile memory cells are based on nanoionic redox processes and offer prospects for high scalability, ultrafast write and read access, and low power consumption. The interfacial electrochemical reactions of oxidation and reduction of ions necessarily needed for resistive switching result inevitably in nonequilibrium states, which play a fundamental role in the processes involved during device operation. We report on nonequilibrium states in SiO_2-based ReRAMs being induced during the resistance transition. It is demonstrated that the formation of metallic cations proceeds in parallel to reduction of moisture, supplied by the ambient. The latter results in the formation of an electromotive force in the range of up to 600 mV. The outcome of the study highlights the hitherto overlooked necessity of a counter charge/reaction to keep the charge electroneutrality in cation-transporting thin films, making it hard to analyze and compare experimental results under different ambient conditions such as water partial pressure. Together with the dependence of the electromotive force on the ambient, these results contribute to the microscopic understanding of the resistive switching phenomena in cation-based ReRAMs.

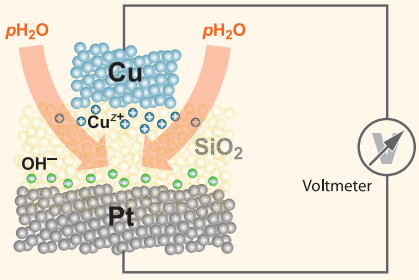

KEYWORDS: redox reactions · electrochemical metalization cell · counter charge · silicon dioxide · electromotive force · ReRAM

To face the upcoming challenges of future information technology, new nonvolatile memory concepts are inevitable to replace conventional flash technology.[1,2] Resistive switching electrochemical metalization (ECM) cells based on redox processes in nanoscaled insulators (*e.g.*, silicon dioxide) attracted high attention due to their low power consumption and high scalability.[3−9] Typically, an ECM cell consists of a working electrode (WE) such as Cu or Ag and a counter electrode (CE) such as Pt separated by an insulating thin film (*e.g.*, SiO_2). Here, the switching effect is contributed by the electrochemical formation and dissolution of a nanoscaled Cu filament within the insulator, short circuiting both electrodes.[10] In contrast to AgI[11] or Ag-GeSe,[12] SiO_2 and many other oxides used as resistive switching films (*e.g.*, Ta_2O_5[13] or WO_3[14]) do not initially contain mobile metal cations (*e.g.*, Cu^+), which are responsible for the filament formation. Thus, one needs first to electrochemically dissolve Cu ions into SiO_2 in order to operate the cell.[15] In this case it is not sufficient to simply apply a positive voltage to the electrochemically active electrode.[16] A counter electrode reaction at the inert electrode must proceed, thus supplying counter charge and allowing the injection of cations into the resistive switching film to maintain the electroneutrality. Failing to ensure a charge transfer reaction at the inert electrode will result in blocking the electrochemical oxidation of the active electrode and will therefore prevent resistive switching. Hence, an appropriate counter reaction/charge is essential for cation-based resistive switching memory (ReRAM) devices using insulating solid films. Water reduction and/or dissociation interacting with SiO_2[17] or with Pt but also oxygen reaction on the Pt electrode may supply the necessary counter reaction (charge) to enable Cu oxidation. Moreover, a distinctive open-circuit voltage (*i.e.*, electromotive force, emf) between the WE and CE electrode was recently measured

* Address correspondence to i.valov@fz-juelich.de.

Received for review May 27, 2013 and accepted June 20, 2013.

Published online June 20, 2013
10.1021/nn4026614

for various ECM material systems including SiO_2[18] and also material systems based on the valency change mechanism such as $SrTiO_3$.[19] The emf was found to be generated by redox reactions involved in the resistive switching process, and the observed effects are similar to those in charging batteries. Being a fundamental part of the redox processes, the discovery of a nonequilibrium state(s) in resistive switches necessitates a crucial amendment to the theoretical treatment of the memristors and memristive devices based on nanoionic resistive switching memories.[18]

While in the literature most attention has been paid to the active electrode, electrochemical reactions at the inert electrode have been widely overlooked. Only a few reports indicate the relevance of reactions occurring at the counter electrode. For instance it has been reported that the switching voltage for SiO_2-based cells during resistance transition from a high resistive state (HRS) to a low resistive state (LRS) increases by a decrease of the water partial pressure.[20] Tsuruoka *et al*. made comprehensive studies on the switching kinetics[21] and the impact of moisture on the switching effect of $Cu/Ta_2O_5/Pt$ and $Cu/SiO_2/Pt$ devices and demonstrated the pronounced impact of ambient moisture on the forming voltage and the switching characteristics of SiO_2-based ECM cells.[22] The increase of the switching voltage in a vacuum was attributed to the removal of water from the nanoporous SiO_2, and the effect of moisture was due to the water-assisted Cu oxidation as well as water-enhanced ion migration along grain boundaries in the oxide layer. However, even though resistive switching in SiO_2 has been intensively studied[23−25] with special attention to the switching kinetics,[26] multibit functionality,[27] or power consumption,[28] the role of a potential counter charge(s) supplied by water or oxygen and their impact on nanoionic-based nonequilibrium states have not been analyzed yet.

Here we report on introducing nonequilibrium states, *i.e.*, chemical potential gradients in the $Cu/SiO_2/Pt$ system, by operating the memory cells. SiO_2 has been selected among several tested oxide-based systems (*e.g.*, Ta_2O_5, TiO_x, WO_3, and HfO_x) showing distinctive advantages as a model system: (i) the system is a purely ECM system (no oxygen vacancy mechanism reported in this operating voltage range) and (ii) the moisture can easily desorb from SiO_2 in dry air and/or vacuum conditions, thus allowing adjusting the water partial pressure within the material (*i.e.*, at the Pt/SiO_2 interface). The nonequilibrium states are affected by the ambient atmosphere and the change of the Cu^{z+} ion concentration at the Cu/SiO_2 interface. As a sequence an electromotive force is generated, strongly influencing the cell performance, and repeatedly renewed during SET/RESET cycles. We emphasize that the effect of the counter charge(s) on the anodic oxidation of Cu is a crucial factor determining the emf

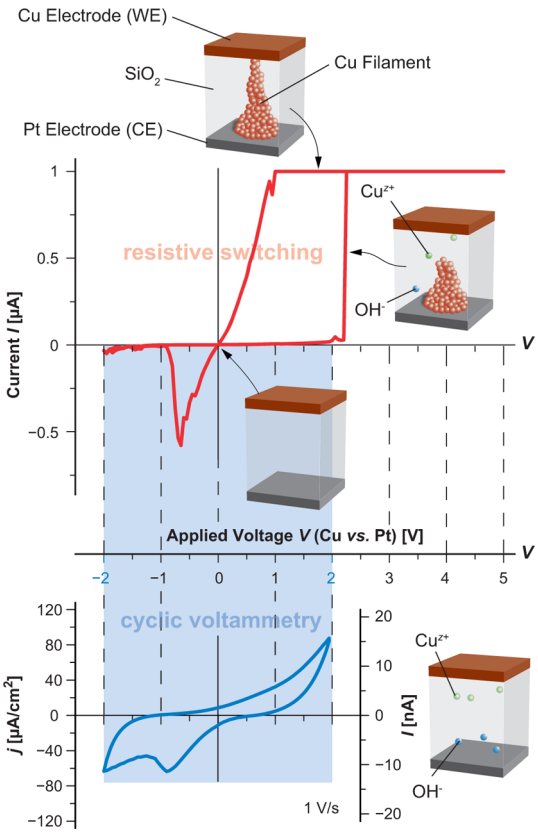

Figure 1. Resistive switching of $Cu/SiO_2/Pt$. The ON resistance strongly depends on the current compliance. In this example $dI/dV \approx 1$ MΩ, dominated by tunneling effects.[39] If the voltage amplitude is limited to ±2 V, resistive switching is avoided and redox processes can be analyzed by cyclic voltammetry (sweep rate 1 V/s). A forming step is not required for cyclic voltammetry. The current is proportional to the electrode diameter. Cyclic voltammetry can also be performed after electroforming. However, in this case, the voltage amplitude needs to be limited to prevent resistive switching.

and is a prerequisite for resistive switching. From X-ray photoelectron spectroscopy (XPS) depth profiles we were able to clearly identify the formation of oxidized Cu species at the Cu/SiO_2 interface after electrode polarization. Electromotive force measurements were then performed to study the impact of water partial pressure, revealing that a water reduction reaction at the Pt electrode provides the counter charge supply required for Cu ion formation at the Cu/SiO_2 interface. Hence, this work significantly contributes to the understanding of the complex mechanism of resistive switching and more generally to the nanoionic redox phenomena involving strongly nonequilibrated states generated by the electrochemical oxidation of Cu.

RESULTS AND DISCUSSION

Resistive Switching and Anodic Oxidation of Cu^{z+} Ions at the Cu/SiO_2 Interface. A detailed view of the resistive switching characteristics and cyclic voltammetry (CV) for comparison is shown in Figure 1. In this context, CV is

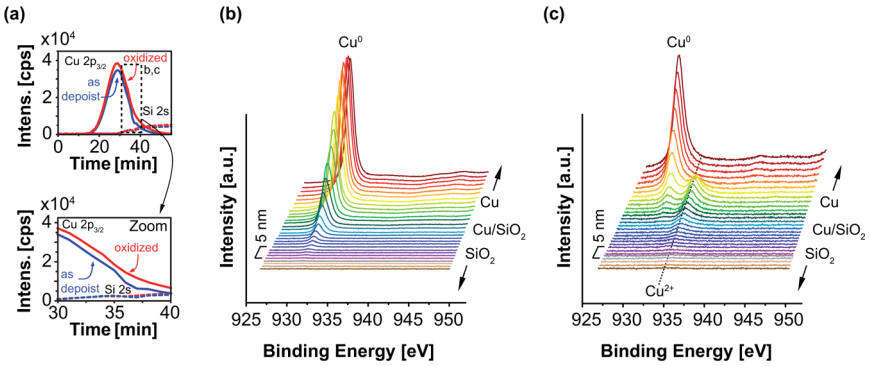

Figure 2. X-ray photoelectron spectroscopy depth profiles. (a) For simplification only the signal response around the binding energy of Cu $2p_{3/2}$ at the Cu/SiO_2 interface is shown (see zoom). (b) XPS spectra shown for the as-deposited sample and (c) after electrochemical oxidation. A clear Cu^{2+} signal appears close to the Cu/SiO_2 interface after oxidation.

a current−voltage sweep method where resistive switching is avoided by limitation of the bias voltage to analyze electrochemical reactions prior to the resistive switching effect. During the positive voltage sweep anodic oxidation of the Cu electrode takes place. Beyond $V > 2$ V the cell switches from the HRS to the LRS and the current is dominated by the highly conducting Cu filament and the current compliance, I_{CC}. By applying a negative voltage the filament is dissolved and the cell is switched back to the HRS. Resistive switching during the positive voltage sweep can be avoided by limitation of the voltage amplitude, revealing the unique opportunity to investigate the redox reactions preceding filament formation (further denoted as cyclic voltammetry experiments, CV). Thus, during the following sweep in a negative voltage regime the reduction processes of the previously oxidized Cu ions close to the WE can be observed in detail.[29] Note, we were not able to observe redox reactions and forming or resistive switching in anhydrous O_2 or N_2 atmospheres.

The formation of Cu ions during electrode polarization is clearly confirmed by XPS depth profiles of Cu/SiO_2/Pt cells in as-deposited state (Figure 2b) as well as after electrochemical oxidation (Figure 2c). The spectra clearly showed the presence of Cu^{2+} ions underneath the Cu electrode in the case of electrode polarization. While cyclic voltammograms reveal the presence of a small amount of Cu^+ ions ($z = 1$) in addition to Cu^{2+} ions,[29] we are not able to clearly distinguish the Cu^+ signal from metallic copper in the XPS profiles due to the small difference in the binding energies. In addition, the resolution and the sensitivity of the method are not sufficient to detect small amounts (below ~1 at. %) of Cu species, and thus, filament formation and/or the existence of a low concentration of Cu ions at the Pt/SiO_2 interface practically cannot be detected. However, the XPS results confirmed the conclusion drawn on the basis of the cyclic voltammogram analysis, where we were able to identify the presence of Cu^{2+} ions.[29] It has been recently reported that according to X-ray absorption spectroscopy measurements, Cu^{2+}−O^{2-} bonds in SiO_2 are much weaker than the Cu^+−O^{2-} bonds, suggesting that Cu^{2+} is more mobile in SiO_2, thus dominating the switching process.[30] It is worth mentioning that the thickness of the interface layer containing Cu^{2+} ions is in the range of a few nanometers, limited by the Cu^{2+} mobility. The estimated relatively small penetration depth indicates that during the switching event Cu ions must be significantly accelerated by the applied field in order to achieve switching times in the microsecond regime or below.[31]

Impact of Moisture on the Cu^{z+} Ion Concentration and Diffusion Coefficient. A counter charge(s)/reaction, *e.g.*, electrons or OH^-, must keep the electroneutrality during device operation. OH^- ions can be supplied by moisture from the surrounding ambient (reaction 2), which is incorporated into SiO_2 because of its nanoporous structure.[22,32] Thus, during the CV sweeps the half-cell reaction at the active electrode is assumed

$$Cu \rightarrow Cu^{2+} + 2e^- \quad (1)$$

and at the inert Pt electrode the required counter reaction is given by

$$\frac{1}{2}O_2 + H_2O + 2e^- \rightarrow 2OH^- \quad (2)$$

To study in detail the impact of moisture on Cu redox processes, we performed CV measurements at different water partial pressures, pH_2O (Figure 3a). Particularly, we analyzed the impact of pH_2O on the concentration of ions (c_{ion}) generated during the sweeping. It must be emphasized that the concentrations of both Cu ions c_{Cu+} and hydroxide ions OH^- (c_{OH-}) are contributing equally to c_{ion}.

The concentration c_{ion} can be estimated by integration of the current during the sweep and the cell geometry. We assume that only one cation species is dominating the switching effect with $z = 2$.[30] In previous studies[15,29] $z = 1$ was used for simplification, resulting in a slightly higher diffusion coefficient.

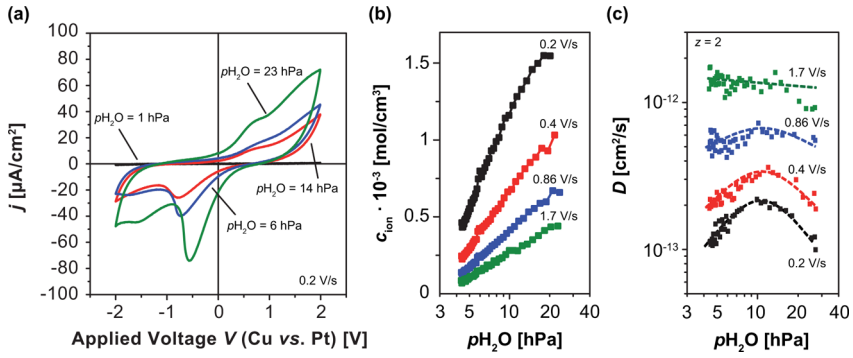

Figure 3. Impact of moisture on Cu^{z+}/Cu redox processes. (a) Cyclic voltammetry in hydrated nitrogen atmosphere (pH_2O = 1 to 23 hPa). (b) Ion concentration (c_{ion}) dependence on pH_2O at constant sweep rates, respectively. The ion concentration was adjusted by variation of the sweep rate[29] and calculated by integration of the anodic oxidation current over time. The ion concentration also depends on the water partial pressure during the anodic oxidation sweep. (c) Diffusion coefficient (D) calculated by the Randles–Sevcik equation and depending on the water partial pressure. The effective diffusion coefficient is decreased at high pH_2O, which is attributed to ion–ion interactions due to high Cu ion concentration. Note, here we assume only one dominating cation species with z = 2.

The diffusion coefficient D is derived as shown in ref 33 using the Randles–Sevcik equation:

$$j_p = (2.99 \times 10^5) z^{3/2} c_{ion} \sqrt{\alpha D \nu} \qquad (3)$$

Here, j_p is the reduction current peak density, ν is the sweep rate, and α = 0.5 the charge coefficient.[29] Increasing of pH_2O during anodic oxidation results in an increase of c_{ion} (Figure 3b) because the introduction of the counter charge at the Pt/SiO_2 interface seems to be the limiting process for anodic oxidation. This relation unequivocally reveals that hydroxide ions are acting as counter charge rather than electrons. At higher water partial pressures more OH^- can be reduced at the Pt/SiO_2 interface and, respectively, a higher amount of Cu^{z+} can be dissolved. Since the high local concentration of Cu ions leads to ion–ion interactions, the thermodynamic factor $\partial \ln a_i / \partial \ln c_i$ (with the activity a_i and the concentration c_i of species i) is reduced, and increasing the partial pressure of water results in a decrease of the diffusion coefficient D (Figure 3c) as in the case typical for concentrated solution conditions.[29] However, the estimated diffusion coefficient for Cu ions is magnitudes of orders higher compared to the extrapolated values in bulk SiO_2 at room temperature.[34] We contribute the higher diffusion coefficient mainly to the nanoporous structure of the deposited SiO_2 layer.[22,32] The diffusion may be additionally increased due to an impact of moisture within the SiO_2 and an electric field enhancement.

The incorporation of charges separated at the both interfaces, *i.e.*, Cu^{z+} at the Cu/SiO_2 interface (I) and OH^- at the SiO_2/Pt interface (II), leads to the formation of an emf within the ECM cell.

Electromotive Force Measurements. Figure 4a depicts the equivalent circuit model of the Cu/SiO_2/Pt cell. The theoretical emf voltage is not directly measured due to the finite electronic partial conductivity (*i.e.*, the mean transference number of ions is not $\bar{t}_{ion}$ = 1). This is represented by the electronic resistance (R_{el}) determined by the leakage current and the ionic resistance (R_i). Thus, the measurable cell voltage (V_{cell}) is given by eq 4:

$$V_{cell} = \bar{t}_{ion} V_{emf} = \frac{{R_i}^{-1}}{{R_i}^{-1} + {R_{el}}^{-1}} V_{emf} \qquad (4)$$

On the basis of Hebb–Wagner polarization measurements[35,36] we found that the transference number for ions is $\bar{t}_{ion}$ = 0.3. The cell voltage of up to V_{cell} = 600 mV strongly depends on the ion concentration (c_{ion}), as shown in Figure 4b. V_{cell} is determined by the emf voltage (V_{emf}), which in turn is composed by both half-cell reactions (Nernst potentials V_N contribution) and a diffusion potential V_d.[18]

$$V_{emf} = V_N + V_d = \underbrace{V^0 + \frac{kT}{2e} \ln \frac{(c_{Cu^{2+}})_I \cdot (c_{OH^-})_{II}^2}{(c_{Cu})_I \cdot (c_{O_2})_{II}^{1/2} \cdot (c_{H_2O})_{II}}}_{V_N} \underbrace{- \frac{kT}{e} \sum_i \int_{II}^{I} \frac{\bar{t}_i}{z_i} \, d \ln c_i}_{V_d} \qquad (5)$$

Here V^0 is the standard potential, k the Boltzmann constant, e the elementary charge, T the absolute temperature, and $\bar{t}_i$ the mean transference number of species i. c_{O_2} is the oxygen concentration (given by pO_2) and c_{H_2O} the water concentration (given by pH_2O) at interface II (SiO_2/Pt). Note, all emf measurements were performed under open-circuit conditions. Possible thermal effects (*i.e.*, thermovoltages) due to high currents during the measurements can be thus safely neglected.

As $c_{ion} = c_{Cu^{z+}} + c_{OH^-}$ increases (by decreasing the sweep rate),[29] the emf increases as well, and thus, a higher value of V_{cell} is measured. A linear slope can be approached when V_{cell} is plotted *versus* log(c_{ion}) (Figure 4c), as evident from eq 4. An emf can also be measured after resistive switching and RESET of the cell. However, the cell voltage is smaller in this case (typically in the range $V_{cell} \approx$ 10–100 mV depending on the sweep rate).

The cell voltage has also been measured at different water partial pressures (pH_2O) in a nitrogen

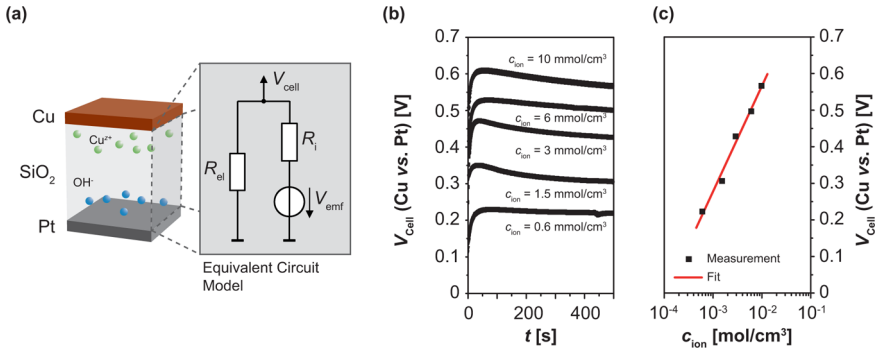

Figure 4. Cell voltage (V_{cell}) between the Cu and Pt electrode analyzed as a function of the ion concentration (c_{ion}). The water partial pressure was kept constant to approximately 4 hPa. (a) Equivalent circuit of the Cu/SiO_2/Pt cell. The cell voltage V_{cell} is determined by the emf voltage V_{emf} and the electronic partial contribution. (b) Transient measurements of V_{Cell} at constant pH_2O for different ion concentrations. Prior to the measurements the ion concentration was adjusted by a single linear anodic oxidation sweep of different sweep rate. (c) V_{cell} dependence on c_{ion}.

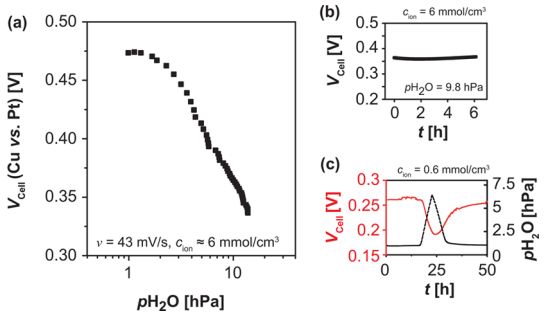

Figure 5. Electromotive force measurement at a constant ion concentration. (a) V_{cell} dependence on the water partial pressure in a nitrogen atmosphere. Each point corresponds to a different pH_2O value. The initial ion concentration (indicated in the plot) was set prior to the measurements. (b) Transient measurement of V_{cell} at constant c_{ion} and pH_2O. (c) V_{cell} (red) response to the variation of the pH_2O (black). The V_{cell} response to pH_2O change is reversible. This indicates that the concentration gradient of Cu remains constant with time and pH_2O does not meaningfully increase the mobility of Cu ions in the SiO_2.

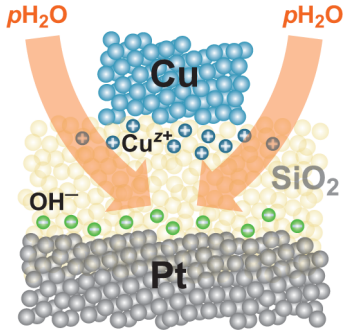

Figure 6. Schematic cross section of the Cu/SiO_2/Pt cell showing the penetration of moisture into the SiO_2 thin film. By changing the water partial pressure (pH_2O) moisture is likely penetrating into the SiO_2 from the lateral sides. The pH_2O equilibration can take several hours depending on the change of ambient water partial pressure. No forming process can be observed in dry atmosphere or in a vacuum below approximately 12 V.

atmosphere, as depicted in Figure 5a. c_{ion} was adjusted prior to the experiment by a single linear anodic oxidation sweep. The ion concentration of both cations and OH^- is believed to be constant during the experiment. From eq 5 it is evident that the emf is influenced by c_{H_2O} (and, thus, pH_2O) also when $c_{Cu^{2+}}$ and c_{OH^-} are constant. To ensure reproducible experimental conditions, the oxygen partial pressure (pO_2) was monitored by an oxygen sensor simultaneously and was found to be constant during the measurements. The highest value for V_{cell} is measured in an anhydrous nitrogen atmosphere. When pH_2O is increased, a decrease of V_{cell} is observed in accordance with eq 5. The system requires at least 60 min relaxation as soon as quasi-equilibrium for each partial pressure of water is reached. Figure 5b shows that V_{cell} remains constant over hours. V_{cell} can be reversibly tuned (increased or decreased) depending on the particular water partial pressure, as depicted in Figure 5c. Hence, pH_2O and, therefore, the water molecules incorporated into SiO_2 do not significantly increase the ion mobility (due to solvent effects), and the Cu^{z+} and OH^- ion concentration gradients and, respectively, the driving force for V_{cell} are not changed.

The results presented above underline the importance of a counter charge/reaction. Without a counter charge/reaction no anodic oxidation can take place, and thus, the resistive switching effect is not observed. We have clearly verified that water is mainly supplying the required counter charge(s) for anodic oxidation and hence resistive switching rather than enhancing the Cu^{z+} ion mobility in SiO_2 thin films, which would result in an irreversible decrease of V_{cell} by increase of pH_2O. Electrons alone seem to play an inferior role as counter charges required for maintaining the electroneutrality because anodic oxidation is not observed in an anhydrous atmosphere.

By XPS depth profiling we observed a pronounced increase of the Cu^{2+} concentration for the electrochemically treated sample in the immediate vicinity of the electrode, whereas the concentration within the SiO_2 film is very small. Thus, we conclude that the half-cell

potential at the working electrode interface (Cu/SiO_2) is defined by the Cu^{z+} ion concentration, and at the counter electrode interface (SiO_2/Pt) the water redox reaction is determining the electrode potential, thus providing the counter charge needed for the Cu half-cell reaction. Increasing the water partial pressure increases the half-cell potential at the counter electrode but lowers the absolute cell potential difference. As soon as water is removed by decreasing pH_2O, the cell voltage (V_{cell}) will increase again in accordance with eq 5.

We assume moisture is likely penetrating from the lateral sides, as depicted in Figure 6. However, resistive switching experiments[20,22] indicate a pH_2O equilibration in the complete SiO_2 thin film, even underneath the top electrodes. This complies with our observation that the V_{cell} equilibration can take up to several hours depending on the change of ambient water partial pressure.

CONCLUSIONS

In this study we have clearly demonstrated by electromotive force measurements that nonequilibrium states are generated by operating ReRAM cells. Without a counter charge/reaction, which is inevitably required to enable anodic oxidation, no resistive switching takes place. Moisture supplying this counter charge/reaction is playing an important role during the electrochemical oxidation of Cu ions, being responsible for the filament formation and, therefore, for resistance transition in SiO_2-based ReRAM cells. The origin of the electromotive force and the impact of pH_2O are attributed to a diffusion potential modulated by the electrochemical half-cell reactions (Nernst potential) at the Cu/SiO_2 and SiO_2/Pt interfaces. The understanding of these effects leads to a new interpretation of the factors controlling the switching behavior in SiO_2-based ECM cells.

METHODS

Platinized p-doped (100) orientated silicon substrates were used for sample fabrication. A 30 nm thick SiO_2 thin film was deposited by electron-beam (e-beam) evaporation at an evaporation speed of 0.01 nm/s. Cu top microelectrodes, 30 nm thick with a diameter of 0.008 to 0.2 mm^2, were prepared by conventional UV lithography and e-beam evaporation of Cu (evaporation speed of 0.025 nm/s). The Cu top electrodes are covered by a 100 nm thick Pt layer to prevent chemical oxidation of the electrode in air. The photoresist was finally removed by lift-off in acetone, 2-propanol, and deionized water. For cyclic voltammetry we applied triangular voltage sweeps between −2 and 2 V at various sweep rates (15 mV/s to 2 V/s) using a Keithley 6430 Sub-Femtoamp remote source meter. The same parameters except from a voltage amplitude of −2 to 5 V were used for resistive switching.[15,33] A Keithley 617 electrometer with high input impedance (>200 TΩ) was used for open-circuit measurements.

The ion concentration at the interfaces has been adjusted by performing a single linear anodic oxidation sweep in a voltage frame from 0 to 2 V. The value for the ion concentration was calculated by integrating the current over the time taking into account the ionic transference number. The variation of the sweep rates between 5 mV/s and 2 V/s results in a different charge and respectively ensures different ion concentrations.

Steady-state emf voltage experiments were performed after the concentration of ions has been adjusted prior to the measurements. We have used a Keithley 617 electrometer and additionally a Keithley 6430 Sub-Femtoamp remote source meter (input impedance $>10^{14}$ Ω) for comparison. We used a triaxial measurement setup and avoided any RFI effects.[37,38] Different water/oxygen partial pressures were achieved in an enclosed measurement chamber using two MKS 179B digital mass flow controllers admixing anhydrous N_2 with anhydrous O_2 or hydrated N_2. The total flow rate through the measurement chamber was kept constant at 100 sccm. The absolute pressure within the measurement chamber was also kept constant close to the ambient absolute pressure using a pressure relief valve. During the measurement the partial pressure of oxygen was measured by a Zirox O_2-DF 12.2 oxygen sensor. The partial pressure of water has been measured using a Honeywell HIH-4000 humidity sensor. The sample temperature (room temperature) was simultaneously monitored.

The XPS spectra were measured at a constant incident angle. For the depth profiling we used Ar sputtering at 3 kV with a sputtering rate lower than 1 nm/min.

Conflict of Interest: The authors declare no competing financial interest.

REFERENCES AND NOTES

1. Waser, R.; Aono, M. Nanoionics-Based Resistive Switching Memories. *Nat. Mater.* **2007**, *6*, 833–840.
2. Waser, R. Resistive Non-Volatile Memory Devices. *Microelectron. Eng.* **2009**, *86*, 1925–1928.
3. Valov, I.; Waser, R.; Jameson, J. R.; Kozicki, M. N. Electrochemical Metallization Memories-Fundamentals, Applications, Prospects. *Nanotechnology* **2011**, *22*, 254003.
4. Valov, I.; Sapezanskaia, I.; Nayak, A.; Tsuruoka, T.; Bredow, T.; Hasegawa, T.; Staikov, G.; Aono, M.; Waser, R. Atomically Controlled Electrochemical Nucleation at Superionic Solid Electrolyte Surfaces. *Nat. Mater.* **2012**, *11*, 530–535.
5. Terabe, K.; Hasegawa, T.; Nakayama, T.; Aono, M. Quantized Conductance Atomic Switch. *Nature* **2005**, *433*, 47–50.
6. Hasegawa, T.; Terabe, K.; Tsuruoka, T.; Aono, M. Atomic Switch: Atom/Ion Movement Controlled Devices for beyond Von-Neumann Computers. *Adv. Mater.* **2012**, *24*, 252–267.
7. Cavallini, M.; Hemmatian, Z.; Riminucci, A.; Prezioso, M.; Morandi, V.; Murgia, M. Regenerable Resistive Switching in Silicon Oxide Based Nanojunctions. *Adv. Mater.* **2012**, *24*, 1197–1201.
8. Kozicki, M. N.; Balakrishnan, M.; Gopalan, C.; Ratnakumar, C.; Mitkova, M. Programmable Metallization Cell Memory Based on Ag-Ge-S and Cu-Ge-S Solid Electrolytes. *Proc. NVMTS* **2005**, 83–89.
9. Yang, Y. C.; Pan, F.; Liu, Q.; Liu, M.; Zeng, F. Fully Room-Temperature-Fabricated Nonvolatile Resistive Memory for Ultrafast and High-Density Memory Application. *Nano Lett.* **2009**, *9*, 1636–1643.
10. Waser, R.; Dittmann, R.; Staikov, G.; Szot, K. Redox-Based Resistive Switching Memories - Nanoionic Mechanisms, Prospects, and Challenges. *Adv. Mater.* **2009**, *21*, 2632–2663.
11. Tappertzhofen, S.; Valov, I.; Waser, R. Quantum Conductance and Switching Kinetics of AgI Based Microcrossbar Cells. *Nanotechnology* **2012**, *23*, 145703.
12. Kozicki, M. N.; Park, M.; Mitkova, M. Nanoscale Memory Elements Based on Solid-State Electrolytes. *IEEE Trans. Nanotechnol.* **2005**, *4*, 331–338.
13. Sakamoto, T.; Lister, K.; Banno, N.; Hasegawa, T.; Terabe, K.; Aono, M. Electronic Transport in Ta_2O_5 Resistive Switch. *Appl. Phys. Lett.* **2007**, *91*, 092110.

14. Kozicki, M. N.; Gopalan, C.; Balakrishnan, M.; Mitkova, M. A Low-Power Nonvolatile Switching Element Based on Copper-Tungsten Oxide Solid Electrolyte. *IEEE Trans. Nanotechnol.* **2006**, *5*, 535–544.
15. Tappertzhofen, S.; Menzel, S.; Valov, I.; Waser, R. Redox Processes in Silicon Dioxide Thin Films Using Copper Microelectrodes. *Appl. Phys. Lett.* **2011**, *99*, 203103.
16. Willis, B. G.; Lang, D. V. Oxidation Mechanism of Ionic Transport of Copper in SiO_2 Dielectrics. *Thin Solid Films* **2004**, *467*, 284–293.
17. Rodriguez, O.; Cho, W.; Saxena, R.; Plawsky, J.; Gill, W. Mechanism of Cu Diffusion in Porous Low-K Dielectrics. *J. Appl. Phys.* **2005**, *98*, 24108.
18. Valov, I.; Linn, E.; Tappertzhofen, S.; Schmelzer, S.; van den Hurk, J.; Lentz, F.; Waser, R. Nanobatteries in Redox-Based Resistive Switches Require Extension of Memristor Theory. *Nat. Commun.* **2013**, *4*, 1771.
19. Saraf, S.; Markovich, M.; Vincent, T.; Rechter, R.; Rothschild, A. Memory Diodes with Nonzero Crossing. *Appl. Phys. Lett.* **2013**, *102*, 22902.
20. Tappertzhofen, S.; Hempel, M.; Valov, I.; Waser, R. Proton Mobility in SiO_2 Thin Films and Impact of Hydrogen and Humidity on the Resistive Switching Effect. *Mater. Res. Soc. Symp. Proc.* **2011**, *1330*, 1–6.
21. Tsuruoka, T.; Hasegawa, T.; Valov, I.; Waser, R.; Aono, M. Rate-Limiting Processes in the Fast SET Operation of a Gapless-Type Cu-Ta_2O_5 Atomic Switch. *AIP Adv.* **2013**, *3*, 32114.
22. Tsuruoka, T.; Terabe, K.; Hasegawa, T.; Valov, I.; Waser, R.; Aono, M. Effects of Moisture on the Switching Characteristics of Oxide-Based, Gapless-Type Atomic Switches. *Adv. Funct. Mater.* **2012**, *22*, 70–77.
23. Yao, J.; Zhong, L.; Zhang, Z.; He, T.; Jin, Z.; Wheeler, P. J.; Natelson, D.; Tour, J. M. Resistive Switching in Nanogap Systems on SiO_2 Substrates. *Small* **2009**, *5*, 2910–2915.
24. Yao, J.; Sun, Z.; Zhong, L.; Natelson, D.; Tour, J. M. Resistive Switches and Memories from Silicon Oxide. *Nano Lett.* **2010**, *10*, 4105–4110.
25. Schindler, C.; Thermadam, S. C. P.; Waser, R.; Kozicki, M. N. Bipolar and Unipolar Resistive Switching in Cu-Doped SiO_2. *IEEE Trans. Electron Devices* **2007**, *54*, 2762–2768.
26. Schindler, C.; Staikov, G.; Waser, R. Electrode Kinetics of Cu-SiO_2-Based Resistive Switching Cells: Overcoming the Voltage-Time Dilemma of Electrochemical Metallization Memories. *Appl. Phys. Lett.* **2009**, *94*, 072109.
27. Bernard, Y.; Renard, V. T.; Gonon, P.; Jousseaume, V. Back-End-of-Line Compatible Conductive Bridging RAM Based on Cu and SiO_2. *Microelectron. Eng.* **2011**, *88*, 814–816.
28. Schindler, C.; Weides, M.; Kozicki, M. N.; Waser, R. Low Current Resistive Switching in Cu-SiO_2 Cells. *Appl. Phys. Lett.* **2008**, *92*, 122910.
29. Tappertzhofen, S.; Mündelein, H.; Valov, I.; Waser, R. Nanoionic Transport and Electrochemical Reactions in Resistively Switching Silicon Dioxide. *Nanoscale* **2012**, *4*, 3040–3043.
30. Cho, D. Y.; Tappertzhofen, S.; Waser, R.; Valov, I. Bond Nature of Active Metal Ions in SiO_2-Based Electrochemical Metallization Memory Cells. *Nanoscale* **2013**, *5*, 1781–1784.
31. Strukov, D. B.; Williams, R. S. Exponential Ionic Drift: Fast Switching and Low Volatility of Thin-Film Memristors. *Appl. Phys. A: Mater. Sci. Process.* **2009**, *94*, 515–519.
32. Kobayashi, Y.; Zheng, W.; Chang, T.; Hirata, K.; Suzuki, R.; Ohdaira, T.; Ito, K. Nanoporous Structure of Sputter-Deposited Silicon Oxide Films Characterized by Positronium Annihilation Spectroscopy. *J. Appl. Phys.* **2002**, *91*, 1704–1706.
33. Bard, A.; Faulkner, L. *Electrochemical Methods: Fundamentals and Applications*; John Wiley and Sons: New York, 2001.
34. McBrayer, J. D.; Swanson, R. M.; Sigmon, Y. W. Diffusion of Metals in Silicon Dioxide. *J. Electrochem. Soc.* **1986**, *133*, 1242–1246.
35. Hebb, M. H. Electrical Conductivity of Silver Sulfide. *J. Chem. Phys.* **1952**, *20*, 185–190.
36. Wagner, C. Proceedings 7th Meeting Lindau 1955. *International Committee of Electrochemical Thermodynamics and Kinetics*; Butterworth Scientific Publications: London, 1957.
37. Keithley Instruments Inc. *Low Level Measurements Handbook*; 2004.
38. Keithley Instruments Inc. *Application Note 312: High Resistance Measurements*; **2005**.
39. Menzel, S.; Böttger, U.; Waser, R. Simulation of Multilevel Switching in Electrochemical Metallization Memory Cells. *J. Appl. Phys.* **2012**, *111*, 014501.